Cell-specific effects of Nox2 on the acute and chronic response to myocardial infarction

Alexander Sirker, Colin E. Murdoch, Andrea Protti, Greta J. Sawyer, Celio X.C. Santos, Daniel Martin, Xiaohong Zhang, Alison C. Brewer, Min Zhang [1], Ajay M. Shah *

King's College London British Heart Foundation Centre of Excellence, Cardiovascular Division, London, UK

ARTICLE INFO

ABSTRACT

Background: Increased reactive oxygen species (ROS) production is involved in the process of adverse cardiac remodeling and development of heart failure after myocardial infarction (MI). NADPH oxidase-2 (Nox2) is a major ROS source within the heart and its activity increases after MI. Furthermore, genetic deletion of Nox2 is protective against post-MI cardiac remodeling. Nox2 levels may increase both in cardiomyocytes and endothelial cells and recent studies indicate cell-specific effects of Nox2, but it is not known which of these cell types is important in post-MI remodeling.

Methods and results: We have generated transgenic mouse models in which Nox2 expression is targeted either to cardiomyocytes (*cardio*-Nox2TG) or endothelial cells (*endo*-Nox2TG). We here studied the response of cardio-Nox2TG mice, *endo*-Nox2TG mice and matched wild-type littermates (WT) to MI induced by permanent left coronary artery ligation up to 4 weeks. Initial infarct size assessed by magnetic resonance imaging (MRI) and cardiac dysfunction were similar among groups. Cardiomyocyte hypertrophy and interstitial fibrosis were augmented in cardio-Nox2TG compared to WT after MI and post-MI survival tended to be worse whereas *endo*-Nox2TG mice showed no significant difference compared to WT.

Conclusions: These results indicate that cardiomyocyte rather than endothelial cell Nox2 may have the more important role in post-MI remodeling.

1. Introduction

Myocardial infarction (MI) is a major cause of heart failure, secondary to progressive adverse left ventricular (LV) remodeling and impairment of contractile function. Adverse cardiac remodeling post-MI is characterized by progressive LV chamber dilatation, interstitial fibrosis, cardiomyocyte hypertrophy in non-infarcted tissue, and decline in contractile performance. An increased production of reactive oxygen species (ROS) and oxidative stress have long been recognized to be involved in the process of post-MI remodeling and heart failure [1–3]. ROS contribute to adverse LV remodeling through multiple mechanisms including detrimental effects on cellular components, impaired energetics, alterations in various redox-sensitive signaling pathways and changes in cardiomyocyte viability.

NADPH oxidases (Noxs) are major ROS sources in the heart, with Nox2 (also known as gp91[phox]) and Nox4 being the two main isoforms that are expressed [4]. Both isoforms require heterodimerization with a p22[phox] subunit but Nox2 additionally requires association with several cytosolic subunits (p47[phox], p67[phox], p40[phox] and Rac1) to manifest full activity [5]. Therefore, Nox2 is acutely activated by agonists that promote the association of cytosolic subunits with the transmembrane Nox2-p22[phox] complex [6] whereas Nox4 activity depends mainly on its abundance [7]. Numerous studies indicate that the activation of Nox2 may contribute to the development of cardiac hypertrophy, interstitial fibrosis and contractile dysfunction in diverse disease situations [8]. Previous studies using gene-modified mice with a global deficiency of Nox2 found that Nox2 contributes to adverse LV remodeling and contractile dysfunction after experimental MI [9,10]. Knockout (KO) mice lacking either Nox2 or p47[phox] were protected against LV dilatation, cardiomyocyte hypertrophy, apoptosis and interstitial fibrosis in the weeks after MI as compared with wild-type (WT) controls [9,10]. This was supported by the finding that Nox2 is upregulated in the infarcted myocardium after acute MI in patients [11] as well as in experimental models [9,10,12–14].

Nox2 in the heart is expressed both in cardiomyocytes and endothelial cells and its activation in these cell types may have different effects [8]. Recently, we have generated transgenic mouse models in which Nox2 is specifically overexpressed either in endothelial cells (*endo*-Nox2TG) [15] or cardiomyocytes (*cardio*-Nox2TG) [16], in order to

study the cell-specific effects of the oxidase. We found that in a model of chronic angiotensin II (AngII) infusion, *endo*-Nox2TG mice developed greater myocardial fibrosis and diastolic LV dysfunction than WT littermates [17]. In *cardio*-Nox2TG mice on the other hand, chronic AngII infusion enhanced contractile function through an increase in sarcoplasmic reticulum (SR) calcium uptake, while more prolonged stress induced by chronic aortic constriction tended to worsen cardiac dysfunction as compared to WT littermates [16]. Therefore, cardiac Nox2 may affect the response to pathological insults in a cell-specific and stress-specific manner. The aim of the current study was to compare the effects of cardiomyocyte versus endothelial Nox2 on the cardiac response to experimental MI.

2. Materials and methods

2.1. Genetically-modified mice and experimental MI

Transgenic mice with cardiomyocyte or endothelium-targeted over-expression of Nox2 (*cardio*-Nox2TG and *endo*-Nox2TG, respectively), both on a C57BL/6 background, were described previously [15,16]. Permanent left coronary artery ligation or sham ligation was performed in female TG mice and matched wild-type littermates (WT) aged 12–18 weeks [9]. All procedures were performed in accordance with the 'Guidance on the Operation of the Animals' (Scientific Procedures) Act, 1986 (UK Home Office) and institutional guidelines.

2.2. Infarct size

Cine-MRI with late Gadolinium enhancement (LGE) was performed 2 days after MI on a 7 T horizontal MR scanner (Varian, Palo Alto, CA) [18]. MRI was repeated at day 28 post-MI (without LGE). The initial infarct area was estimated from the day 2 LGE images using a semi-automated in-house developed segmentation software (King's College London, www.clinicalvolumes.com) [19]. Infarct area was expressed as a percentage of total LV area and only animals with an infarct area >30% were included in the study. Infarct size at 4 week follow-up was estimated using infarct arc lengths rather than areas to avoid underestimation relating to infarct thinning and compensatory non-infarct hypertrophy, as previously described [20]. LV volumes and ejection fraction (EF) were derived as described previously [19].

2.3. Echocardiography and in vivo LV hemodynamics

Echocardiography was performed under 2% isoflurane anesthesia at heart rates >400 bpm, using a Vevo 2100 system with a 40 MHz linear probe (Visualsonics, Canada) [16]. LV end diastolic volume (LVEDV), LV end systolic volume (LVESV) and EF were measured using the parasternal long axis view. Peak longitudinal strain of basal LV segments was analyzed by high-frequency speckle tracking [21].

In vivo LV hemodynamics were determined by closed-chest pressure-volume (PV) analysis using a 1.2F microconductance catheter system (Scisense Inc., London, Ontario, Canada) introduced retrogradely into the LV via the right carotid artery under 2% isoflurane anesthesia (body temperature 37 °C). After stabilization, data were acquired via an ADVantage™ system (Scisense Inc., London, Ontario, Canada) coupled to a Powerlab/8SP with Chart Software (ADinstruments, UK). Analysis was conducted using Labscribe, IWork Systems Inc., Dover, NH [17].

2.4. Real-time RT-PCR

Total RNA was purified from non-infarct LV tissue using an SV RNA extraction kit (Promega, UK). Expression of atrial natriuretic factor (ANF), brain natriuretic peptide (BNP), beta-myosin heavy chain (β-MHC), α-myosin heavy chain (α-MHC), connective tissue growth factor (CTGF), fibronectin, matrix metallopeptidase 2 (MMP2), and tissue inhibitor of metalloproteinase 2 (TIMP2) mRNA was analyzed by real-time RT-PCR using SYBR Green on an Applied Biosystem PRISM 7700 machine, with β-actin as an internal control. Standard curves were constructed from cDNA standards for each gene, and results were normalized by expression as a molar/molar ratio to β-actin. The primers used were (5′-3′): β-actin forward CGTGAAAAGATGACCCAGATCA, reverse TGGTACGACCAGAGGCATACAG; ANF forward CGTGCCCCGACCCACGCCAGCATGGGCTCC, reverse GGCTCCGAGGGCCAGCGAGCAGAGCCCTCA; BNP forward AAGGGAGAATACGGCATCATTG, reverse ACAGCACCTTCAGGAGATCCA; β-MHC forward AGCAGCAGTTGGATGAGCGACT, reverse CCAGCTCCTCGATGCGTGCC; α-MHC forward TAAAATTGAGGACGAGCAGGC, reverse TCCAGCTCCTCGATGCGT; CTGF forward GCTGCCTACCGACTGGAAGAC, reverse GAACAGGCGCTCCACTCTG; fibronectin forward CCGGTGGCTGTCAGTCAGA, reverse CCGTTCCCACTGCTGATTTATC; MMP2 forward TCGCCCATCATCAAGTTCCC, reverse CCTTGGGGCAGCCATAGAAA and TIMP2 forward GGTACCAGATGGGCTGTGA, reverse CATCCAGAGGCACTCATCCG.

2.5. Histology

Non-infarcted basal LV segments from hearts arrested in diastole were fixed in 1% paraformaldehyde and embedded on paraffin blocks and onto slides. Cardiomyocyte cross-sectional area was measured from sections stained with FITC-conjugated wheat germ agglutinin (WGA, Vector RL-1022) [22]. Interstitial fibrosis was assessed by blinded quantitative image analysis of Picrosirius red-stained sections [16]. Collagen content was quantified as the percentage of total LV area under polarized light. Apoptosis was determined by terminal deoxynucleotidyl transferase–mediated dUTP nick end-labelling (TUNEL) staining according to the manufacturer's instructions (Roche Applied Science). The number of apoptotic myocytes was counted, and data were normalized per 10^5 total nuclei identified by DAPI staining in the same sections [9].

2.6. ROS levels

Superoxide levels in heart tissue were quantified using high-performance liquid chromatography (HPLC)-based detection of dihydroethidium (DHE) oxidation products [23]. Briefly, hearts harvested from mice were cut into small pieces, weighed and immediately incubated with DHE (100 μM in PBS) at 37 °C for 30 min. The sample was then washed once with PBS. DHE and its oxidation products were extracted with acetonitrile (500 μl), sonicated (3 × 30 s, 8 W), centrifuged (14,000 rpm, 10 min at 4 °C) and the supernatant dried under vacuum. The samples were further dissolved in 120 μl PBS-DTPA and injected into the HPLC system. The specific superoxide oxidation product, 2-hydroxyethidine (EOH), was quantified by comparison of peak signal between the samples and standard solutions under identical chromatographic conditions. Results are expressed as the ratio of EOH generated per DHE consumed (initial DHE concentration minus remaining DHE; EOH/DHE).

As a second method, we quantified tyrosine nitrosylated proteins as an index of nitroso-oxidative modification, by immunoblotting using an anti-nitrotyrosine antibody (Abcam; 1:3000). Levels were normalized by the level of actin in the same samples.

2.7. Statistics

Data are expressed as mean ± SEM of at least 3 independent experiments. Kaplan Meier survival curves were compared using the log rank test. Other data were analyzed by unpaired Student *t*-test, 1-way or 2-way ANOVA as appropriate, followed by Tukey post hoc analysis. $p < 0.05$ was considered significant.

3. Results

3.1. Infarct size and survival

Infarct area measured 48 h after MI by MRI LGE was not different between groups (Fig. 1A). Infarct size evaluated by MRI correlated well with that by triphenyltetrazolium chloride (TTC) staining (data not shown). Infarct area assessed at 4 weeks post-MI (as the thinned akinetic area on MRI) was also similar in endo-Nox2TG and cardio-Nox2TG as compared to their respective WT littermates (Fig. 1A). The infarct areas both at early and late time points were comparable to our previous studies [9]. Fig. 1B shows Kaplan Meier curves over a 4 week period and indicates that mortality rate was slightly although non-significantly higher in cardio-Nox2TG mice than WT, while survival rates in endo-Nox2TG were identical to those in WT mice.

3.2. LV dilatation and dysfunction

LV end-diastolic volume (LVEDV) assessed by echocardiography increased significantly over the 4 weeks period after MI, but there were no difference between the two TG groups and respective WT animals in the extent of LV dilatation (Fig. 2A and E). LVEF also decreased to a similar extent in both TG groups and WT controls (Fig. 2B and F). Heart rates were similar among groups (Fig. 2C and G). Similar results were

obtained by MRI (data not shown). To look for more subtle changes in LV contractile function, we used high frequency speckle tracking analysis [21]. The peak systolic longitudinal strain of LV basal non-infarcted segments was significantly reduced in mice 4 weeks post-MI, but there were no differences between the cardio-Nox2TG or endo-Nox2TG and their respective WT controls (Fig. 2D and H).

3.3. LV hemodynamics

We assessed contractile function by in vivo cardiac catheterization. Both LV dP/dt_{max} and LV $dP/dt_{max}/LVEDV$ - measures of systolic function - were decreased 4 weeks after MI but to a similar extent in all groups (Fig. 3A, B, E and F). LV dP/dt_{min} and the isovolumic relaxation time constant, τ, as measures of diastolic function were also impaired after MI but again there was no significant difference between TG and WT (Fig. 3C, D, G and H).

3.4. ROS levels, cardiomyocyte hypertrophy, fibrosis and apoptosis

Myocardial superoxide levels assessed by HPLC of DHE oxidation products increased after MI both in cardio-Nox2TG mice and their WT littermates but the increase was significantly greater in the former group (Fig. 4A). In line with this, the protein levels of nitrotyrosine were significantly higher in cardio-Nox2TG mice than WT after MI
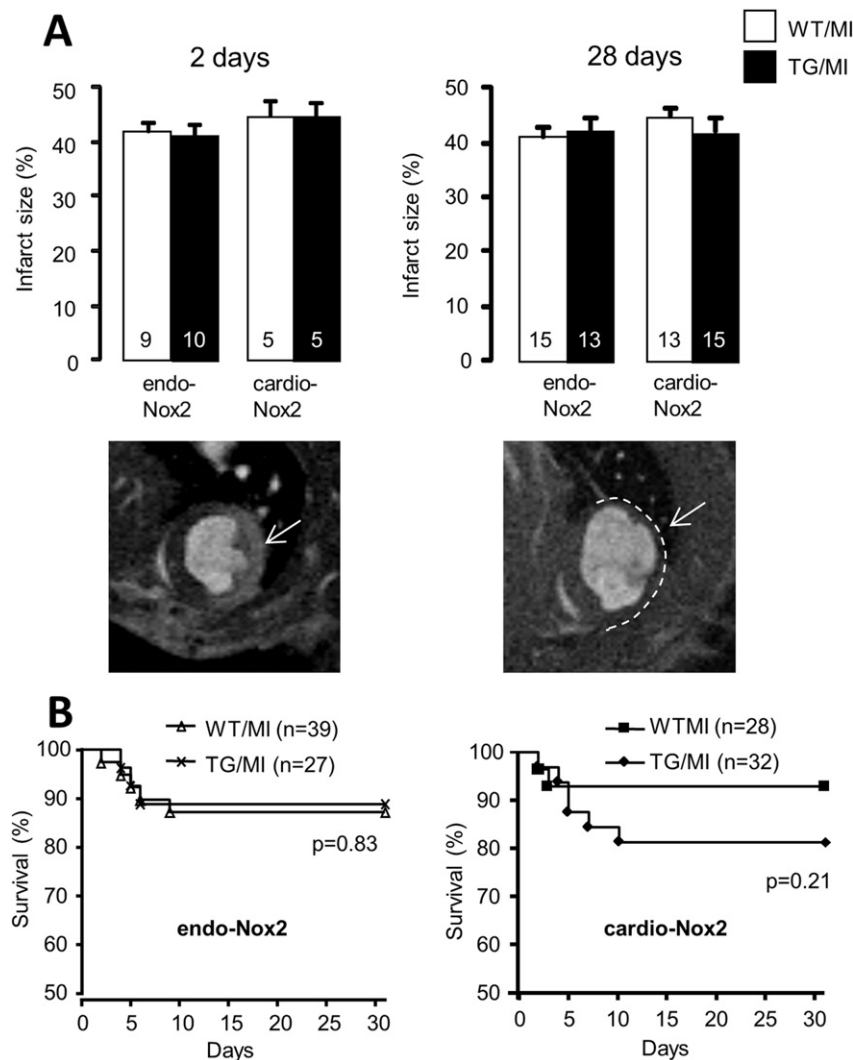

Fig. 1. Infarct size and survival rate post-MI. A. Infarct size assessed by MRI at 2 days and 4 weeks post-MI. Representative MRI images are shown below; arrows indicate infarct area by LGE at 2 days and area of infarct scar at 4 weeks post-MI. B. Kaplan Meier survival curves for endo-Nox2TG, cardio-Nox2TG and respective WT controls after MI.
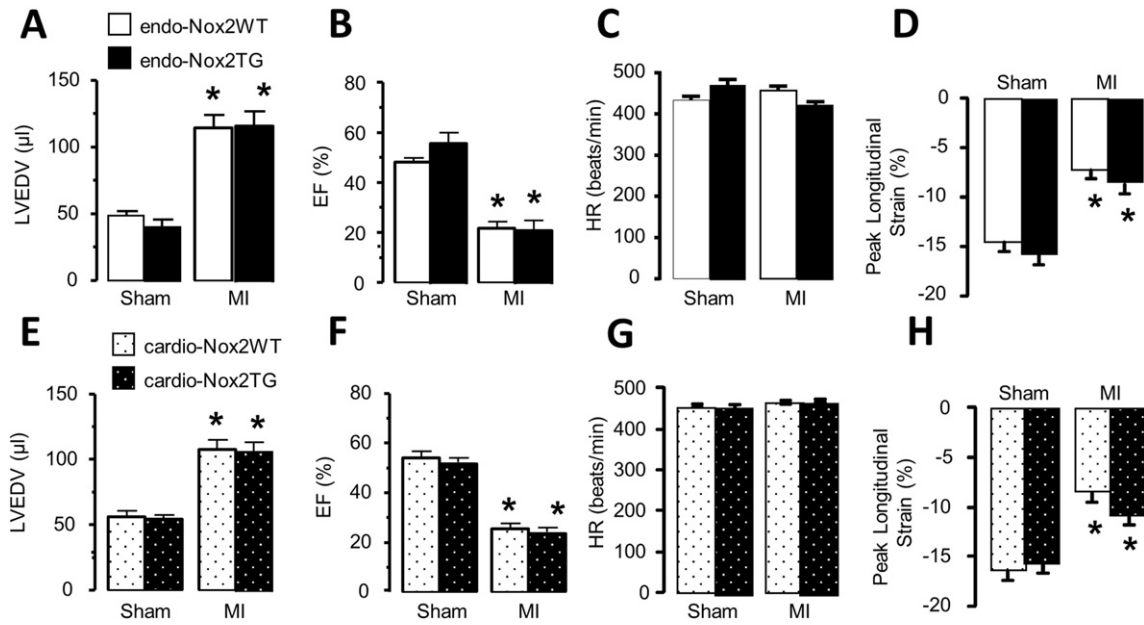
Fig. 2. LV volume and function after MI as assessed by echocardiography. LVEDV, left ventricle end diastolic volume; EF, ejection fraction; HR, heart rate. *$p < 0.05$ vs respective sham controls. $n = 5$–9/group for endo-Nox2TG, $n \geq 7$/group for cardio-Nox2TG.

(Fig. 4B). The cardiomyocyte cross-sectional area in the remote myocardium increased after MI, and the increase was significantly higher in cardio-Nox2TG mice than WT (Fig. 4C, Supplementary Fig. 1A). ANF mRNA expression levels, as a molecular marker of hypertrophy, also tended to increase more in cardio-Nox2TG than WT (Fig. 4D). Other hypertrophic markers, namely BNP and β-MHC increased after MI while α-MHC decreased, but the responses were similar in cardio-Nox2TG mice and WT littermates (Supplementary Fig. 1B–D). Interstitial fibrosis increased after MI, with a significantly higher increase in cardio-Nox2TG mice compared to WT (Fig. 4E, Supplementary Fig.1E). The mRNA levels of CTGF, fibronectin and the matrix-regulating enzymes MMP2 and TIMP2 were similar between groups (Supplementary Fig. 1F–I). The

level of cardiomyocyte apoptosis was similarly increased in cardio-Nox2TG and WT hearts post-MI (Fig. 4F).

In the endo-Nox2TG group, the myocardial levels of superoxide and protein levels of nitrotyrosine increased after MI to a similar extent as in WT littermates (Fig. 5A, B). We also found a similar increase in endo-Nox2TG and WT groups in myocyte cross-sectional area (Fig. 5C, Supplementary Fig. 2A) and ANF mRNA levels (Fig. 5D). Other molecular markers of hypertrophy were no different between groups (Supplementary Fig. 2B–D). The degree of interstitial fibrosis and mRNA levels of fibrotic markers and matrix-regulating proteins were similar between endo-Nox2TG and WT after MI (Fig. 5E, F and Supplementary Fig. 2E–H).
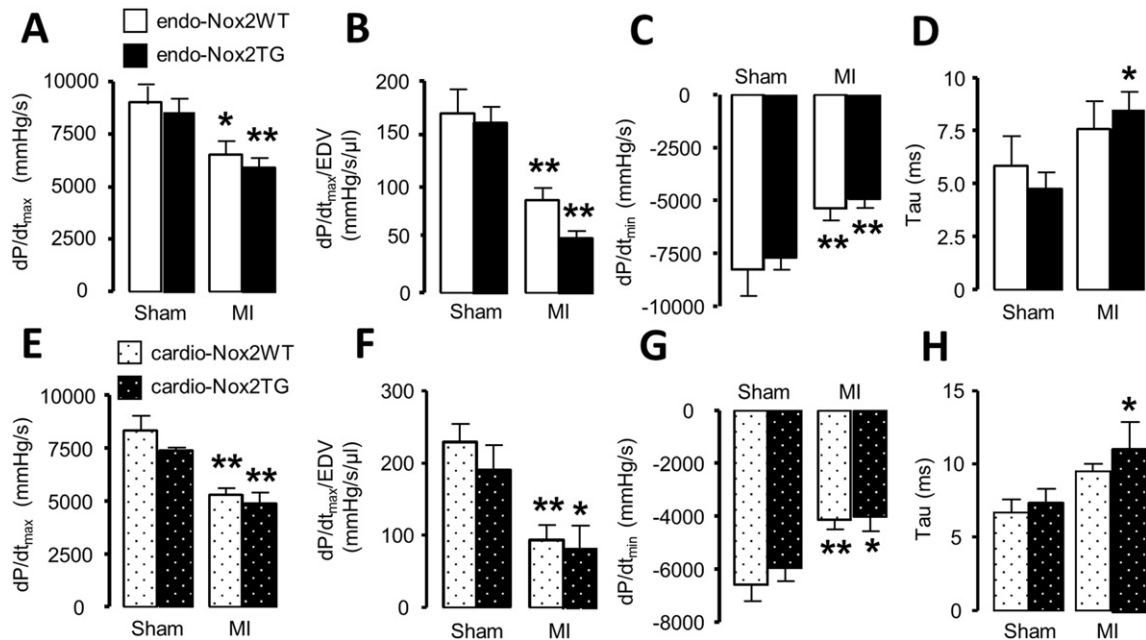

Fig. 3. LV hemodynamics after MI. LVdP/dtmax, LVdP/dtmax/LVEDV, LVdP/dtmin and isovolumic relaxation time constant tau are shown. *$p < 0.05$, **$p < 0.01$ vs respective sham controls. $n = 4$–8/group.
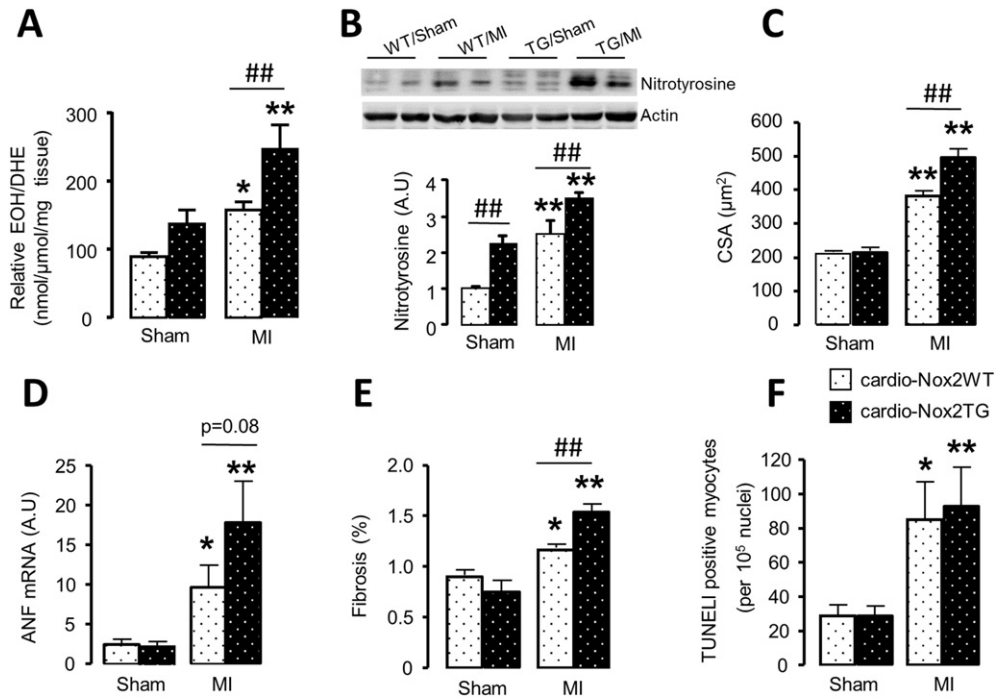
Fig. 4. ROS production, cardiomyocyte cross-sectional area (CSA), interstitial fibrosis and apoptosis after MI in *cardio*-Nox2TG mice. (A) Levels of superoxide in the heart assessed by HPLC analysis of DHE oxidation product EOH. (B) Protein levels of nitrotyrosine assessed by Western blot. (C) Mean data for cardiomyocyte area and (E) interstitial fibrosis. (D) Atrial natriuretic factor (ANF) mRNA expression. (E) TUNEL-positive cells. *$p < 0.05$, **$p < 0.01$ vs respective sham controls. ## $p < 0.01$ vs WT/MI, $n = 4$–7/group.

Thus, *cardio*-Nox2TG mice develop more remodeling (hypertrophy and fibrosis) of the non-infarct myocardium than do the *endo*-Nox2TG mice or WT animals, effects which are accompanied by higher ROS levels in the *cardio*-Nox2TG mice than WT.

4. Discussion

Increasing evidence indicates that enhanced ROS production and oxidative stress are involved in post-MI remodeling, contributing to cell
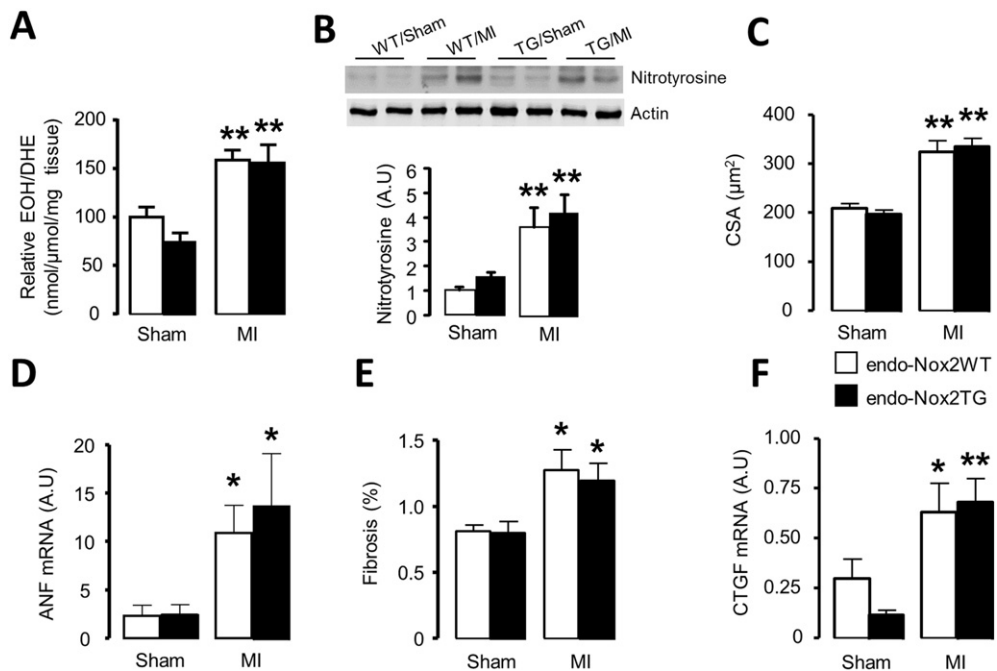

Fig. 5. ROS production, cardiomyocyte cross-sectional area (CSA) and interstitial fibrosis after MI in *endo*-Nox2TG mice. (A) Levels of superoxide in the heart assessed by HPLC analysis of DHE oxidation product EOH. (B) Protein levels of nitrotyrosine assessed by Western blot. (C) Mean data for cardiomyocyte area and (E) interstitial fibrosis. (D) Atrial natriuretic factor (ANF) and (F) Connective tissue growth factor (CTGF) mRNA expression. *$p < 0.05$, **$p < 0.01$ vs respective sham controls. $n = 4$–7/group.

death and inflammation in the early phases and to cardiomyocyte hypertrophy, fibrosis, LV chamber dilatation and contractile dysfunction in the late phase after MI [24]. Several ROS sources may in principle contribute to ROS production, for example mitochondria, uncoupled nitric oxide synthases, xanthine oxidases and NADPH oxidases. Among these sources, Nox2 is especially implicated in adverse LV remodeling based on previous findings from several different types of study. The levels of Nox2 increase 1.5–4 fold in the infarct region and the remote myocardium after MI, both in experimental models and in humans [10–14]. The global deletion of Nox2 or its regulatory subunit p47^{phox} was found to reduce the extent of MI-induced adverse remodeling, heart failure and rupture [9,10,25]. Furthermore, agents that inhibit Nox2 oxidase activity such as apocynin and statins have been found to have beneficial effects on adverse post-MI LV remodeling [26–28]. Local delivery of siRNA to silence Nox2 could also improve cardiac function following MI [29]. These studies clearly indicate that an increase in Nox2 levels and activity after MI contribute to detrimental LV remodeling. Since Nox2 is expressed both in the endothelium and in cardiomyocytes, and recent studies indicate cell-specific effects [16,17,30], it is of interest to identify the impact Nox2 in these cell types has during the response to MI. In this study, we took advantage of two transgenic models recently developed in our laboratory in which the levels of Nox2 are modestly (2–5-fold) increased in either the cardiomyocyte or the endothelium [15,16]. This level of increase in Nox2 is in a pathophysiologically relevant range, being similar to levels previously reported in the literature [10,13,14]. Importantly, it was shown in these models that levels of other oxidase complex components were not affected by this modest level of increase in Nox2 nor were there changes in antioxidant genes [15,16]. These models therefore allowed us to investigate the cell-specific effects of Nox2 during post-MI LV remodeling.

We found that an increase in cardiomyocyte Nox2 levels resulted in significantly greater cardiomyocyte hypertrophy and interstitial fibrosis in the remote myocardium after MI as compared to WT littermate mice, indicating that cardiomyocyte Nox2 aggravates this aspect of the LV remodeling response. These effects were accompanied by evidence of significantly higher ROS levels in *cardio*-Nox2Tg myocardium than WT. These results indicate that cardiomyocyte Nox2 aggravates hypertrophy and fibrosis post-MI and are in line with previous studies that demonstrated a Nox2-ROS-mediated enhancement of cultured cardiomyocyte hypertrophy [31,32], and that Nox2 promotes cardiac fibrosis [33]. The mechanisms involved in the hypertrophic effects included a Nox2-mediated enhancement of ERK1/2 and Akt signaling in cardiomyocytes, while mechanisms promoting fibrosis included the production of connective tissue growth factor (CTGF), NF-κB signaling and MMP activation [31–33]. We observed increases in ANF mRNA levels in *cardio*-Nox2Tg mice compared to WT after MI but other molecular markers of hypertrophy and genes potentially involved in fibrosis were not different between groups. This may be because the extent of increase in hypertrophy and fibrosis was relatively modest and changes in gene expression may have been transient. We also did not observe a difference in LV dysfunction between *cardio*-Nox2 Tg mice and WT but the Tg group tended to have a higher mortality after MI. Our transgenic mice have quite modest increases in Nox2 activity [16] and it is likely that a greater increase in Nox2 might result in detrimental effects also on LV contractile function.

In contrast to the *cardio*-Nox2TG mice, we found that *endo*-Nox2TG showed no differences from WT in any parameter after MI. While the lack of effect on cardiomyocyte hypertrophy was expected (because Nox2 was overexpressed in endothelial cells), our previous study in these mice in a model of chronic angiotensin II stimulation showed that endothelial Nox2 can enhance endothelial-mesenchymal transition, fibrosis and diastolic dysfunction [17]. However, we found no evidence in the present study of either enhanced fibrosis or worse diastolic dysfunction after MI in these mice. In line with this, although myocardial ROS levels rose after MI, there was no difference between the extent of increase in *endo*-Nox2Tg mice and WT littermates. This finding

indicates that the effects of endothelial Nox2 may depend upon the stress stimulus and there may be a differential activation of endothelial versus cardiomyocyte Nox2 after MI.

Increasing data indicates that the effects of ROS depend not only upon the enzymatic source but also the cell type(s) within which they are generated. This is especially so for ROS effects that involve the modulation of intracellular signaling pathways. The current results suggest that cardiomyocyte rather than endothelial Nox2 has the greater impact on adverse remodeling after MI. These results add to the evidence that the pathophysiological effects of Noxs are isoform-specific, cell-specific and context-specific. This complexity will be important to bear in mind in developing therapeutic approaches that target the detrimental effects of Noxs in the heart.

Disclosures

None.

Appendix A. Supplementary data

Supplementary data to this article can be found online at http://dx.doi.org/10.1016/j.yjmcc.2016.07.003.

References

[1] Y.T. Sia, N. Lapointe, T.G. Parker, J.N. Tsoporis, C.F. Deschepper, A. Calderone, et al., Beneficial effects of long-term use of the antioxidant probucol in heart failure in the rat, Circulation 105 (2002) 2549–2555.

[2] S. Kinugawa, H. Tsutsui, S. Hayashidani, T. Ide, N. Suematsu, S. Satoh, et al., Treatment with dimethylthiourea prevents left ventricular remodeling and failure after experimental myocardial infarction in mice : role of oxidative stress, Circ. Res. 87 (2000) 392–398.

[3] T. Shiomi, H. Tsutsui, H. Matsusaka, K. Murakami, S. Hayashidani, M. Ikeuchi, et al., Overexpression of glutathione peroxidase prevents left ventricular remodeling and failure after myocardial infarction in mice, Circulation 109 (2004) 544–549.

[4] B. Lassègue, A. San Martín, K.K. Griendling, Biochemistry, physiology, and pathophysiology of NADPH oxidases in the cardiovascular system, Circ. Res. 110 (2012) 1364–1390.

[5] J.D. Lambeth, Nox enzymes and the biology of reactive oxygen, Nat. Rev. Immunol. 4 (2004) 181–189.

[6] R.K. Ambasta, P. Kumar, K.K. Griendling, H.H.H.W. Schmidt, R. Busse, R.P. Brandes, Direct interaction of the novel Nox proteins with p22phox is required for the formation of a functionally active NADPH oxidase, J. Biol. Chem. M406486200 (2004).

[7] L. Serrander, L. Cartier, K. Bedard, B. Banfi, B. Lardy, O. Plastre, et al., NOX4 activity is determined by mRNA levels and reveals a unique pattern of ROS generation, Biochem. J. 406 (2007) 105–114.

[8] M. Zhang, A. Perino, A. Ghigo, E. Hirsch, A.M. Shah, NADPH oxidases in heart failure: poachers or gamekeepers? Antioxid. Redox Signal. 18 (2013) 1024–1041.

[9] Y.H. Looi, D.J. Grieve, A. Siva, S.J. Walker, N. Anilkumar, A.C. Cave, et al., Involvement of Nox2 NADPH oxidase in adverse cardiac remodeling after myocardial infarction, Hypertension 51 (2008) 319–325.

[10] C. Doerries, K. Grote, D. Hilfiker-Kleiner, M. Luchtefeld, A. Schaefer, S.M. Holland, et al., Critical role of the NAD(P)H oxidase subunit p47phox for left ventricular remodeling/dysfunction and survival after myocardial infarction, Circ. Res. 100 (2007) 894–903.

[11] P.A.J. Krijnen, C. Meischl, C.E. Hack, C.J.L.M. Meijer, C.A. Visser, D. Roos, et al., Increased Nox2 expression in human cardiomyocytes after acute myocardial infarction, J. Clin. Pathol. 56 (2003) 194–199.

[12] T. Fukui, M. Yoshiyama, A. Hanatani, T. Omura, J. Yoshikawa, Y. Abe, Expression of p22-phox and gp91-phox, essential components of NADPH oxidase, increases after myocardial infarction, Biochem. Biophys. Res. Commun. 281 (2001) 1200–1206.

[13] B. Li, J. Tian, Y. Sun, T.R. Xu, R.F. Chi, X.L. Zhang, et al., Activation of NADPH oxidase mediates increased endoplasmic reticulum stress and left ventricular remodeling after myocardial infarction in rabbits, Biochim. Biophys. Acta (BBA) - Mol. Basis Dis. 1852 (2015) 805–815.

[14] J. Xu, Y. Sun, O.A. Carretero, L. Zhu, P. Harding, E.G. Shesely, et al., Effects of cardiac overexpression of the angiotensin II type 2 receptor on remodeling and dysfunction in mice post myocardial infarction, Hypertension 63 (2014) 1251–1259.

[15] C. Murdoch, S. Alom-Ruiz, M. Wang, M. Zhang, S. Walker, B. Yu, et al., Role of endothelial Nox2 NADPH oxidase in angiotensin II-induced hypertension and vasomotor dysfunction, Basic Res. Cardiol. (2011) 1–12.

[16] M. Zhang, B.L. Prosser, M.A. Bamboye, A.N.S. Gondim, C.X. Santos, D. Martin, et al., Contractile function during angiotensin-IIÂ activation: increased Nox2 activity modulates cardiac calcium handling via phospholamban phosphorylation, J. Am. Coll. Cardiol. 66 (2015) 261–272.

[17] C.E. Murdoch, S. Chaubey, L. Zeng, B. Yu, A. Ivetic, S.J. Walker, et al., Endothelial NADPH oxidase-2 promotes interstitial cardiac fibrosis and diastolic dysfunction through Proinflammatory effects and endothelial-mesenchymal transition, J. Am. Coll. Cardiol. 63 (2014) 2734–2741.

[18] A. Protti, X. Dong, A. Sirker, R. Botnar, A.M. Shah, MRI-based prediction of adverse cardiac remodeling after murine myocardial infarction, Am. J. Physiol. Heart Circ. Physiol. 303 (2012) H309–H314.

[19] A. Protti, A. Sirker, A.M. Shah, R. Botnar, Late gadolinium enhancement of acute myocardial infarction in mice at 7T: cine-FLASH versus inversion recovery, J. Magn. Reson. Imaging 32 (2010) 878–886.

[20] J. Takagawa, Y. Zhang, M.L. Wong, R.E. Sievers, N.K. Kapasi, Y. Wang, et al., Myocardial infarct size measurement in the mouse chronic infarction model: comparison of area- and length-based approaches, J. Appl. Physiol. 102 (2007) 2104–2111.

[21] A. Bhan, A. Sirker, J. Zhang, A. Protti, N. Catibog, W. Driver, et al., High-frequency speckle tracking echocardiography in the assessment of left ventricular function and remodeling after murine myocardial infarction, Am. J. Physiol. Heart Circ. Physiol. 306 (2014) H1371–H1383.

[22] M. Zhang, A.C. Brewer, K. Schröder, C.X. Santos, D.J. Grieve, M. Wang, et al., NADPH oxidase-4 mediates protection against chronic load-induced stress in mouse hearts by enhancing angiogenesis, PNAS 107 (2010) 18121–18126.

[23] R. Ray, C.E. Murdoch, M. Wang, C.X. Santos, M. Zhang, S. Alom-Ruiz, et al., Endothelial Nox4 NADPH oxidase enhances vasodilatation and reduces blood pressure in vivo, Arterioscler. Thromb. Vasc. Biol. 31 (2011) 1368–1376.

[24] Y. Sun, Oxidative stress and cardiac repair/remodeling following infarction, Am. J. Med. Sci. 334 (2007) 197–205.

[25] B.J. He, J. Ml, M.V. Singh, E.D. Luczak, P.D. Swaminathan, O.M. Koval, et al., Oxidation of CaMKII determines the cardiotoxic effects of aldosterone, Nat. Med. 17 (2011) 1610–1618.

[26] F. Qin, M. Simeone, R. Patel, Inhibition of NADPH oxidase reduces myocardial oxidative stress and apoptosis and improves cardiac function in heart failure after myocardial infarction, Free Radic. Biol. Med. 43 (2007) 271–281.

[27] J. Bauersachs, P. Galuppo, D. Fraccarollo, M. Christ, G. Ertl, Improvement of left ventricular remodeling and function by hydroxymethylglutaryl coenzyme A reductase inhibition with cerivastatin in rats with heart failure after myocardial infarction, Circulation 104 (2001) 982–985.

[28] S. Hayashidani, H. Tsutsui, T. Shiomi, N. Suematsu, S. Kinugawa, T. Ide, et al., Fluvastatin, a 3-hydroxy-3-methylglutaryl coenzyme A reductase inhibitor, attenuates left ventricular remodeling and failure after experimental myocardial infarction, Circulation 105 (2002) 868–873.

[29] I. Somasuntharam, A.V. Boopathy, R.S. Khan, M.D. Martinez, M.E. Brown, N. Murthy, et al., Delivery of Nox2-NADPH oxidase siRNA with polyketal nanoparticles for improving cardiac function following myocardial infarction, Biomaterials 34 (2013) 7790–7798.

[30] J.K. Bendall, R. Rinze, D. Adlam, A.L. Tatham, J. de Bono, K.M. Channon, Endothelial Nox2 overexpression potentiates vascular oxidative stress and hemodynamic response to angiotensin II, Circ. Res. 100 (2007) 1016–1025.

[31] L. Xiao, D.R. Pimentel, J. Wang, K. Singh, W.S. Colucci, D.B. Sawyer, Role of reactive oxygen species and NAD(P)H oxidase in alpha(1)-adrenoceptor signaling in adult rat cardiac myocytes, Am. J. Physiol. Cell Physiol. 282 (4) (2002) C926–C934.

[32] S.D. Hingtgen, X. Tian, J. Yang, S.M. Dunlay, A.S. Peek, Y. Wu, R.V. Sharma, J.F. Engelhardt, R.L. Davisson, Nox2-containing NADPH oxidase and Akt activation play a key role in angiotensin II-induced cardiomyocyte hypertrophy, Physiol. Genomics 26 (3) (2006) 180–191.

[33] S. Johar, A.C. Cave, A. Narayanapanicker, D.J. Grieve, A.M. Shah, Aldosterone mediates angiotensin II-induced interstitial cardiac fibrosis via a Nox2-containing NADPH oxidase, FASEB J. 20 (9) (2006) 1546–1548.